TI 2009-041/4
Tinbergen Institute Discussion Paper

Dynamic Factor Models with Smooth Loadings for Analyzing the Term Structure of Interest Rates

Borus Jungbacker[a]
Siem Jan Koopman[a,c]
Michel van der Wel[b,c,d,e]

[a] *VU University Amsterdam;*
[b] *Erasmus University Rotterdam;*
[c] *Tinbergen Institute;*
[d] *ERIM;*
[e] *CREATES, Aarhus.*

Tinbergen Institute

The Tinbergen Institute is the institute for economic research of the Erasmus Universiteit Rotterdam, Universiteit van Amsterdam, and Vrije Universiteit Amsterdam.

Tinbergen Institute Amsterdam
Roetersstraat 31
1018 WB Amsterdam
The Netherlands
Tel.: +31(0)20 551 3500
Fax: +31(0)20 551 3555

Tinbergen Institute Rotterdam
Burg. Oudlaan 50
3062 PA Rotterdam
The Netherlands
Tel.: +31(0)10 408 8900
Fax: +31(0)10 408 9031

Smooth Dynamic Factor Analysis with an Application to the U.S. Term Structure of Interest Rates

Borus Jungbacker[(a)] *Siem Jan Koopman*[(a,b)] *Michel van der Wel*[(b,c)]

[(a)] Department of Econometrics, VU University Amsterdam

[(b)] Tinbergen Institute

[(c)] Erasmus School of Economics, ERIM Rotterdam and CREATES, Aarhus

September 14, 2010

Some keywords: Fama-Bliss data set; Kalman filter; Maximum likelihood; Yield curve.
JEL classification: C32, C51, E43.

Acknowledgements: We would like to thank Francis X. Diebold and Dick van Dijk for their comments on an earlier version of this paper. Furthermore, we have benefited from the comments by conference participants of the 10th Econometric Society World Congress in Shanghai (August 2010), the 16th International Conference on Panel Data at University of Amsterdam (July 2010), the International Symposium on Econometric Theory and Applications at Singapore Management University (April 2010), the 2nd Amsterdam-Bonn workshop in Econometrics at Tinbergen Institute (May 2010), the Yield Curve Modeling workshop at Econometric Institute of the Erasmus University Rotterdam (June 2010), the Econometric Society European Meetings (ESEM) in Barcelona (August 2009) and the 3rd International Conference on Computational and Financial Econometrics in Limassol, Cyprus (October 2009), and from participants of seminars at CREATES of Aarhus University (April 2009) and Federal Reserve Board in Washington DC (March 2010). Further details of our estimation procedure and its results reported in this paper are available from the authors upon request. Possible remaining errors are our own. Michel van der Wel acknowledges the support from CREATES, funded by the Danish National Research Foundation.

Address of correspondence: S.J. Koopman, Department of Econometrics, VU University Amsterdam, De Boelelaan 1105, NL-1081 HV Amsterdam, The Netherlands.
Emails: bjungbacker@feweb.vu.nl s.j.koopman@feweb.vu.nl vanderwel@ese.eur.nl

Smooth Dynamic Factor Analysis with an Application to the U.S. Term Structure of Interest Rates

Borus Jungbacker, Siem Jan Koopman and Michel van der Wel

Abstract

We consider the dynamic factor model and show how smoothness restrictions can be imposed on the factor loadings. Cubic spline functions are used to introduce smoothness in factor loadings. We develop statistical procedures based on Wald, Lagrange multiplier and likelihood ratio tests for this purpose. A Monte Carlo study is presented to show that our procedures are successful in identifying smooth loading structures from small sample panels. We illustrate the methodology by analyzing the U.S. term structure of interest rates. An empirical study is carried out using a monthly time series panel of unsmoothed Fama-Bliss zero yields for treasuries of different maturities between 1970 and 2009. Dynamic factor models with and without smooth loadings are compared with dynamic models based on Nelson-Siegel and cubic spline yield curves. All models can be regarded as special cases of the dynamic factor model. We carry out statistical hypothesis tests and compare information criteria to verify whether the restrictions imposed by the models are supported by the data. Out-of-sample forecast evidence is also given. Our main conclusion is that smoothness restrictions on loadings of the dynamic factor model for the term structure can be supported by our panel of U.S. interest rates and can lead to more accurate forecasts.

1 Introduction

The general dynamic factor model increasingly plays a major role in econometrics. Early contributions to the literature on dynamic factor models can be found in Sargent and Sims (1977), Geweke (1977), Engle and Watson (1981), Watson and Engle (1983), Connor and Korajczyk (1993) and Gregory, Head, and Raynauld (1997). Most of these papers consider time series panels with limited panel dimensions. The increasing availability of high dimensional data sets has intensified the quest for computationally efficient estimation methods. The strand of literature headed by Forni, Hallin, Lippi, and Reichlin (2000), Stock and Watson (2002) and Bai (2003) led to a renewed interest in dynamic factor analysis. These methods are typically applied to high dimensional panels of time series. Exact maximum likelihood methods such as proposed in Watson and Engle (1983) have traditionally been dismissed as computationally too intensive for such high dimensional panels. An exception is the study by Quah and Sargent (1993) who consider a moderately sized panel of economic time series in their study. Jungbacker and Koopman (2008) however present new results that facilitate application of exact maximum likelihood methods for very high dimensional panels. Examples of recent papers employing likelihood-based methods for the analysis of dynamic factor models are Doz, Giannone, and Reichlin (2006) and Reis and Watson (2010).

In this paper we develop an econometric likelihood-based framework for the introduction of smoothness in the factor loadings of a dynamic factor model. The smoothness conditions on the loadings are first introduced via spline functions that depend on knot coefficients, see Poirier (1976). We develop next statistical procedures based on Wald, Lagrange multiplier and likelihood ratio tests for finding a suitable set of restrictions. General to specific and specific to general approaches are discussed and compared with each other. Monte Carlo evidence is provided to show that smoothness conditions can be detected accurately while some preference is given to the specific to general approach of determining the smoothness in factor loadings. The idea of imposing smoothness in loadings has earlier been considered by Fengler, Haerdle, and Schmidt (2002) in an application of analyzing volatility in financial markets. Their approach is recently developed further using semiparametrics methods by Park, Mammen, Haerdle, and Borak (2009). Here we develop a full maximum likelihood procedure for imposing smoothness in the factor structure.

There are several motivations to impose smoothness on the factor loadings in a dynamic factor model. The economic motivation of smooth loadings is to establish an interpretation for the factors. When the factor loadings are related to particular characteristics of the corresponding variables in the panel, we can impose this relationship by specifying a smooth flexible function for the factor loading coefficients. A smooth pattern in a column of the

loading matrix can lead to an interpretable factor that is associated with this column. In our empirical study for a panel of interest rates, we impose smoothness on the loadings through a spline function that depends on time to maturity. The common interpretation of the factors as level, slope and curvature of the yield curve can be established. Also in other cases a smooth relationship between the underlying factors and observations may exist. Our model could therefore be applied in other applications, including modelling volatility and analyzing electricity prices. The econometric motivation of smooth loadings is the aim for a parsimonious model specification where individual loading coefficients are interpolated by a flexible function that depends on a small number of coefficients. The precision of parameter estimates is generally increased by considering more parsimonious models. Furthermore, smoothness in factor loadings may also lead to models that are more robust to aberrant observations. It is also often argued that forecasts based on a model with a small set of parameters can be expected to be more precise than those based on a less parsimonious model; see the discussion in Clements and Hendry (1998). We develop a flexible new method for introducing smoothness in the loadings for each dynamic factor in the model.

To empirically investigate whether our method of imposing smoothness restrictions on factor loadings is effective, we analyze a panel of U.S. interest rate series for different times to maturity. In the modelling of interest rates it is common to assume that the term structure of different maturities (or yield curve) is driven by a small set of unobserved stochastic factors. In this paper we consider the general dynamic factor model for analyzing the term structure of interest rates. The yield curve tends to be a smooth function of time to maturity. It is therefore reasonable to assume that the factor loadings are smooth functions of time to maturity as well. The primary aim of our paper is to find empirical evidence to support the assumption of smooth factor loadings. For this purpose, we consider the dynamic factor model with and without smoothness, together with two alternative model specifications.

The alternative model specifications are the dynamic Nelson-Siegel model and the functional signal plus noise model. The first model for the term structure is based on the seminal paper of Nelson and Siegel (1987) in which the yield curve is approximated by a weighted sum of three smooth functions. The form of these three functions depends on a single parameter. Diebold and Li (2006) use the Nelson-Siegel framework to develop a two-step procedure for the forecasting of future yields. They show that forecasts obtained from this procedure are competitive with forecasts obtained from other standard prediction methods. Diebold, Rudebusch, and Aruoba (2006) integrate the two-step approach into a single dynamic factor model by specifying the Nelson-Siegel weights as an unobserved vector autoregressive process. A generalization of their state space approach is considered by Koopman, Mallee, and Van der Wel (2010), who allow the parameter governing the shape of the Nelson-Siegel func-

tions to be time-varying and who allow for the inclusion of conditional heteroskedasticity for the innovations in the model. Due to its popularity amongst practitioners, central bankers and academics, the Nelson-Siegel model serves as our benchmark term structure model. The dynamic Nelson-Siegel model can also be regarded as a special case of the dynamic factor model and we compare it with our smooth dynamic factor model in the empirical study. The second model is recently discussed by Bowsher and Meeks (2008) and represents the term structure as a cubic spline function that is observed with measurement noise. The parameters controlling the shape of the spline are time-varying and modelled as a cointegrated vector autoregressive process with different numbers of lags. We consider a basic version of this model and also compare it with the other models in our empirical study that focuses both on in-sample and out-of-sample results. Related work on factor structures in the term structure of interest rates has appeared recently. For example, Duffee (2009) studies restrictions on general factor models of the term structure imposed by arbitrage relationships with a focus on forecasting performance while Lengwiler and Lenz (2010) develop a factor model for the yield curve in which the innovations of the factors are mutually orthogonal. This paper considers smoothness in dynamic factor models generally. While our empirical study concerns the yield curve, our framework can be applied in different circumstances as well.

The empirical study is considering a newly constructed monthly time series panel of unsmoothed Fama-Bliss zero yields for U.S. treasuries of different maturities between 1970 and 2009. The data set is used to empirically validate the aforementioned models. Our main empirical finding is that the dynamic factor model without restrictions on the factor loadings is able to fit the yield curve very accurately. In other words, the standard errors of the estimated factor loadings are small overall. This finding implies that for imposing smoothing restrictions on the factor loadings, the smoothing functions must be sufficiently flexible to closely match the smooth loadings with the unrestricted loadings. Although likelihood ratio tests reject all considered restricted dynamic factor models, the likelihood of our smooth dynamic factor model is closest to the likelihood of the unrestricted model while the Schwarz information criterion indicates that it is the preferred dynamic factor model. We also investigate the forecasting ability of the considered models. Our smooth dynamic factor model produces forecasts that are more accurate than those for the unrestricted model, for most maturities and forecasting horizons. Also when we compare our forecasts with those of the dynamic Nelson-Siegel and the functional plus signal models, the accuracy of our forecasts are generally higher. Nevertheless, the forecasts produced by the different models do not deviate much from each other. We can conclude that our proposed statistical procedure for constructing a parsimonious dynamic factor model with smooth factor loadings has favourable in-sample and out-of-sample properties.

The structure of the paper is as follows. The general dynamic factor model is presented and discussed in section 2. In this section we further develop our methodology to construct dynamic factor models with smooth factor loadings and some simulation evidence is given of its effectiveness in small samples. Section 3 presents and discusses the results of our extensive empirical study for the U.S. term structure of interest rates. Section 4 concludes and provides suggestions for future research.

2 The smooth dynamic factor model

We consider a time series panel of N variables with the observation at time t given by the $N \times 1$ vector

$$y_t = (y_{1t}, \ldots, y_{Nt})', \qquad t = 1, \ldots, n,$$

where y_{it} is the observation for the ith variable in the panel, at time t. The vector of all observations in the panel is denoted by $y = (y_1', \ldots, y_n')'$. The general dynamic factor model is given by

$$y_t = \mu_y + \Lambda f_t + \varepsilon_t, \qquad \varepsilon_t \sim \text{NID}(0, H), \qquad t = 1, \ldots, n, \tag{1}$$

where μ_y is an $N \times 1$ vector of constants, Λ is the $N \times r$ factor loading matrix, f_t is an r-dimensional stochastic process, ε_t is the $N \times 1$ disturbance vector and H is an $N \times N$ variance matrix. The Gaussian disturbance vector series ε_t is serially uncorrelated as NID refers to normally and independently distributed. We further assume that the variance matrix of the observation disturbances H is diagonal. It implies that the covariance between the variables in y_t depends solely on the latent factor f_t. The factor f_t is treated as a signal generated from a linear dynamic process and it can be specified as

$$f_t = Z\alpha_t, \tag{2}$$

where the fixed $r \times p$ matrix Z relates f_t with the p-dimensional unobserved state vector α_t which is modelled by the dynamic stochastic process

$$\alpha_{t+1} = \mu_\alpha + T\alpha_t + R\,\eta_t, \qquad \eta_t \sim \text{NID}(0, Q), \qquad t = 1, \ldots, n, \tag{3}$$

with $p \times 1$ vector of constants μ_α, $p \times p$ transition matrix T and $p \times q$ selection matrix R (consists typically of ones and zeros). The $q \times 1$ disturbance vector η_t has $q \times q$ variance matrix Q and is uncorrelated with ε_s for all $s, t = 1, \ldots, n$. Although dimensions N, p, q and r can be chosen freely, here we consider models which typically have $r \leq p$, $p \geq q$

and $N >> r$. The vectors μ_y and μ_α and the matrices Λ, H, Z, T and Q are referred to as system matrices. This general dynamic factor model can be regarded as a specific case of the state space model. Its statistical treatment is based on the Kalman filter and maximum likelihood in which the initial state conditions are treated properly; see, among others, Durbin and Koopman (2001). The typical dynamic specification for f_t is the vector autoregressive process which can be represented in the form of (2)–(3); see, for example, Box, Jenkins, and Reinsel (1994). The inclusion of lagged factors in the observation equation (1) can also be established in this form; see Appendix.

The elements of the system matrices may depend on unknown parameters that need to be estimated. To ensure identification we need to impose restrictions on the parameters in the mean vectors μ_y and μ_α together with those in Λ, T and Q that govern the covariance structure. The main concern of this paper is the inference on the loading matrix Λ and therefore we prefer to avoid additional restrictions on the remaining parameters. Hence we set $\mu_\alpha = 0$ and estimate μ_y as this is the most general specification. Restrictions on Λ are needed because only its column space can be identified uniquely. Several restrictions on Λ can be considered. For example, we can select r rows of Λ and set these equal to subsequent rows of the $r \times r$ identity matrix I_r. When the first r rows are set equal to I_r, we interpret the elements of f_t as being the first three variables in y_t subject to observation noise in ε_t. Such restrictions for Λ allow us to leave the parameters in T and Q unrestricted.

2.1 Parameter estimation and signal extraction

The dynamic factor model consisting of (1), (2) and (3), is a special case of the linear state space model. For given values of the system matrices, we can use the Kalman filter and related methods to evaluate minimum mean square linear estimators (MMSLE) of the state vector at time t given the observation sets $\{y_1, \ldots, y_{t-1}\}$ (prediction), $\{y_1, \ldots, y_t\}$ (filtering) and $\{y_1, \ldots, y_n\}$ (smoothing). A detailed treatment of state space methods is given by Durbin and Koopman (2001). The Kalman filter can also be used to evaluate the loglikelihood function via the prediction error decomposition. The maximum likelihood estimators of the model parameters can then be obtained by numerical optimization. To generate the results in this paper we used the BFGS algorithm to perform the optimization, see for example Nocedal and Wright (1999). An alternative approach would be to use the EM algorithm as developed for state space models by Watson and Engle (1983).

Computationally efficient versions of the Kalman filter have been developed for multivariate models, see for example, Koopman and Durbin (2000). Furthermore, we can achieve considerable computational savings using the methods of Jungbacker and Koopman (2008).

Their method first maps the set of observations y_t into a set of vectors which have the same dimensions as the latent factors f_t in (2). We can then apply the Kalman filter to a typically lower dimensional "observation" vector. We have implemented this approach in our analysis. These efficient Kalman filter methods are also used to evaluate the closed form expressions for the score function given in Koopman and Shephard (1992). Despite of the large number of parameters involved, this combination of efficient Kalman filter methods and analytical score computations allows us to estimate the parameters for all models in a matter of seconds.

2.2 Smooth loadings

The main assumption of our smooth dynamic factor model is that the loading coefficients in Λ of the dynamic factor model (1) are subject to smoothing restrictions. We assume that the jth column of Λ can be represented by a smooth interpolating function. Different smoothness functions can be considered. Many classes of interpolating functions rely on a selection of knots in the range of some variable x that is associated with the vector variable y_t. Then, the scalar x_i represents a particular characteristic of the ith variable in y_t, for $i = 1, \ldots, N$. For example, x_i can be a measure of size, location or maturity associated with variable y_{it}. We can enforce the restrictions that the same loading coefficients for variables with x_i in a particular range of values (for example, small, medium and large sizes, when x_i represents the size of the ith variable). Alternatively, we can linearly interpolate the loading coefficient between, say, three knot values that are placed at the smallest possible x-value (small size), an intermediate x-value (medium size) and the largest possible x-value (large size). In both case we reduce the estimation of N coefficients in a column of Λ to a small number of coefficients that equals the number of groups or the number of knots (in the example, three). For the interpolation of the loading coefficients in each column of Λ, we adopt the cubic spline function as discussed by Poirier (1976) and Monahan (2001). The cubic spline function is similar to a linear interpolation method but it behaves more flexibly. It is a third-order polynomial between the knots and it is twice continuously differentiable at the knots. We assume that for each column in Λ, an x variable is selected and its values are known or observed for each ith variable in y_t, with $i = 1, \ldots, N$. The x variable can be different for different columns of Λ. We also assume that the variable x_i does not change with time-index t although this assumption is not necessary for the implementation of our method. The number and location of knots for the x variable determine the smoothness of the spline function In our empirical study of section 3, we have y_{it} as the interest rate of an U.S. bond and x_i as the time to maturity of the bond, for all columns in Λ.

In the developments below, we follow the cubic spline representation of Poirier (1976) closely. In our case, it allows expressing the loading coefficients as linear functions of the coefficients associated with the knots (groups). For the jth column of Λ, we assume that a particular x variable is chosen and that the number of knots is set to k_j. The cubic spline interpolation for the coefficients in the jth column of Λ is then given by

$$\Lambda_{ij} = w_{ij}'\bar{\lambda}_j, \qquad w_{ij} = w(x_i, \bar{x}_1, \ldots, \bar{x}_{k_j}), \tag{4}$$

where Λ_{ij} is the (i,j) element of loading matrix Λ in (1), the $k_j \times 1$ vector w_{ij} contains the spline weights and $k_j \times 1$ vector of coefficients $\bar{\lambda}_j$ contains the coefficients associated with the knots. The spline weights in vector w_{ij} are determined by the actual value of x_i, the k_j knot positions and the restrictions associated with the cubic spline being a third-order polynomial and being twice continuously differentiable at the knots, see Monahan (2001). When $x_i = \bar{x}_m$, the weight vector w_i is equal to the mth column of the identity matrix I_{k_j}, for any $m = 1, \ldots, k_j$. The first and last knot positions, $\bar{x}_1$ and $\bar{x}_{k_j}$, represent the minimum and maximum of all possible x values, respectively. In vector notation, we can represent the smooth loadings by

$$\Lambda_j = W_j'\bar{\lambda}_j, \tag{5}$$

where Λ_j is the jth column of Λ and $k_j \times N$ matrix of spline weights $W_j = (w_{1j}, \ldots, w_{Nj})$ and with w_{ij} defined as in (4). Instead of estimating the individual coefficients in the jth column Λ_j, we estimate the smaller set of coefficients in $\bar{\lambda}_j$. For each column Λ_j, we can determine a different x variable, a different number of knots k_j, a different set of knots $\bar{x}_1, \ldots, \bar{x}_k$ and a different coefficient vector $\bar{\lambda}_j$.

When a small number of knots k_j is chosen, the factor loadings in the jth column of Λ exhibit a highly smooth pattern. In our approach it is not necessary that all columns Λ are smooth. When the number of knots is equal to N, we have $k_j = N$ and w_{ij} reduces to the ith column of the identity matrix I_N such that $N \times 1$ vector $\bar{\lambda}_j$ contains all coefficients for the jth column of Λ. As a result, no smoothness restrictions are imposed on the factor loadings in Λ_j.

2.3 Smooth signal

The signal of the observation equation (1) is defined as $\mathrm{E}(y_t|f_t) = \mu_y + \Lambda f_t$. In this section we mainly focus on the time-varying part Λf_t. Smooth loading vectors in Λ can lead to a smooth signal Λf_t. When all loading vectors $\Lambda_1, \ldots, \Lambda_r$ are smooth, the signal vector $\Lambda f_t = \sum_{j=1}^{r} \Lambda_j f_{jt}$, with f_{jt} as the jth element of f_t, is also smooth because a weighted sum

of smooth vectors is smooth. So far we have adopted a cubic spline function for each column of Λ. We can also use the cubic spline to obtain a smooth signal vector Λf_t directly. In this case, we substitute Λf_t in (1) by the term $W'\bar{f}_t$ where W is a spline weights matrix as W_j defined in (5) and based on a selection of r^* knots with the $r^* \times 1$ time-varying coefficient vector $\bar{f}_t$. The coefficients in $\bar{f}_t$ represent the knot coefficients as those of $\bar{\lambda}_j$ in (5) with the major difference that we let the knot coefficients be directly time-varying as f_t and specified as in (2) and (3). This is the approach taken by Harvey and Koopman (1993) for the modelling and forecasting of hourly electricity load consumption curves and it is further explored in the context of modelling the yield curve of interest rates by Bowsher and Meeks (2008). The time-varying cubic spline signal $W'\bar{f}_t$ is clearly more parsimonious since all parameters in Λ have disappeared but the factors in $\bar{f}_t$ do not have the interpretation that can be the result of the (smooth) structure in Λ.

We can regard the cubic spline signal as a restricted version of our smooth loadings framework. When the knot positions for the cubic spline functions for each column in Λ_j and for the signal $W'\bar{f}_t$ are placed at the same locations, we have $W_j = W$ and $r = r^*$. Given (5), the signal vector reduces to

$$\Lambda f_t = \sum_{j=1}^{r} \Lambda_j f_{jt} = \sum_{j=1}^{r} W_j' \bar{\lambda}_j f_{jt} = W' \sum_{j=1}^{r} \bar{\lambda}_j f_{jt} = W' \bar{f}_t,$$

with the equality $\bar{f}_t = \sum_{j=1}^{r} \bar{\lambda}_j f_{jt}$. Hence the cubic spline signal can be the result of adding further restrictions to signals from a dynamic factor model with smooth loadings only. We can formulate an appropriate null hypothesis to carry out a test whether the signal can be expressed as a cubic spline signal. This discussion is extended in the context of our empirical illustration in section 3.5.

2.4 Selecting knots: general to specific via Wald

In this section we develop our first statistic to test if a subset of knots is significantly contributing to model fit. We use this test statistic to systematically search for a suitable set of restrictions for the loading matrix Λ in the smooth dynamic factor model. Our first procedure starts from an unrestricted loading matrix and looks for suitable restrictions.

Suppose we have for each column Λ_j selected a number of knots k_j and a set of knots $X_j = \{\bar{x}_1, \ldots, \bar{x}_{k_j}\}$ for $j = 1, \ldots, r$. The knot positions in $X_1, \ldots, X_r$ are sufficiently rich to capture the form of Λ from the set of coefficient vectors $\bar{\lambda} = \{\bar{\lambda}_1, \ldots, \bar{\lambda}_r\}$. More formally, we denote $\Lambda(X_j)$ as the family of cubic spline functions that generates the jth column of Λ in the true data generating process and that is based on X_j, for $j = 1, \ldots, r$. Our aim is to

test whether a subset of knots can be removed from a given set X_j. Consider a new set of k_j^* knots denoted by X_j^* such that X_j^* is a subset of X_j, that is $X_j^* \subset X_j$, and therefore $k_j^* < k_j$. The family of splines determined by the knots in X_j^* is denoted by $\Lambda(X_j^*)$. It follows that $\Lambda_j^* \subset \Lambda_j$. For our purpose, the null-hypothesis H_0 and the alternate hypothesis H_1 are given by

$$H_0 : W_j'\bar{\lambda}_j \in \Lambda(X_j^*), \qquad H_1 : W_j'\bar{\lambda}_j \notin \Lambda(X_j^*), \tag{6}$$

with W_j as in (5) based on X_j. The null-hypothesis is specifically for the jth spline or the jth column of Λ. It can be extended to more general settings and to all r splines jointly.

Each spline function in Λ_j is uniquely determined by the value of $\bar{\lambda}_j$. Similarly, Λ_j^* is uniquely determined by the vector $\bar{\lambda}_j^*$ which contains the coefficients associated with the knots in X_j^*. The null-hypothesis can therefore be written as

$$H_0 : W_j'\bar{\lambda}_j = W_j^{*\prime}\bar{\lambda}_j^*, \tag{7}$$

where the $k_j^* \times N$ matrix W_j^* is defined as matrix W_j in (6) but is based on X_j^* instead of X_j. Under the null-hypothesis, the spline function $W_j^{*\prime}\bar{\lambda}_j^*$ is an element of Λ_j and therefore we can also write it in terms of W_j, that is

$$H_0 : W_j'\bar{\lambda}_j = (W_{j*}', W_{j+}')\bar{\lambda}_j^\dagger, \qquad \bar{\lambda}_j^\dagger = \begin{pmatrix} \bar{\lambda}_j^* \\ \bar{\lambda}_j^+ \end{pmatrix}, \tag{8}$$

where the $k_j^* \times N$ matrix W_{j*} consists of the rows in W_j associated with the knots in X_j^*, the remaining rows of W are collected in W_{j+} and the corresponding coefficients are placed in the auxiliary $(k_j - k_j*) \times 1$ vector $\bar{\lambda}_j^+$. Given that, (i) the spline function is uniquely determined by the knots and its coefficient values, and (ii) the columns of W_j at the knot positions X_j are equal to the subsequent columns of the identity matrix I_{k_j}, then, under the null-hypothesis, the equality of the splines on the right-hand-sides of (7) and (8) holds if

$$\bar{\lambda}_j^+ = W_{j/*}^{*\prime}\bar{\lambda}_j^* \tag{9}$$

where $(k_j - k_j^*) \times k_j^*$ matrix $W_{j/*}^*$ consists of the columns of W_j^* associated with the knots in X_j but not in X_j^*.

Given the result in (9), we can rewrite the null-hypothesis by the $k_j - k_j^*$ restrictions

$$H_0 : R_j\bar{\lambda}_j^\dagger = 0, \qquad \text{where } R_j = (I_{k_j - k_j^*}, -W_{j/*}^*). \tag{10}$$

Testing linear restrictions of the form (10) is standard in the context of maximum likelihood estimation; see, for example, Engle (1984). For our purposes, a Wald test can be convenient. Denote $\widehat{\bar{\lambda}}_j^{\dagger}$ as the maximum likelihood estimator of $\bar{\lambda}_j^{\dagger}$ and $\widehat{V}_j$ as a consistent estimator of the asymptotic variance of $\sqrt{nN}(\widehat{\bar{\lambda}}_j^{\dagger} - \bar{\lambda}_j^{\dagger})$. Under the null-hypothesis we then have

$$n \cdot N \cdot \widehat{\bar{\lambda}}_j^{\dagger\prime} R_j'(R_j \widehat{V}_j R_j')^{-1} R_j \widehat{\bar{\lambda}}_j^{\dagger} \overset{a.}{\sim} \chi^2\left(k_j - k_j^*\right), \tag{11}$$

where $k_j - k_j^*$ is the number of restrictions imposed under the null-hypothesis. In practice a suitable estimator $\widehat{V}_j$ can be constructed from the Hessian matrix of the loglikelihood function evaluated at the maximum likelihood estimator for $\bar{\lambda}_j^{\dagger}$.

An important special case of (11) is the situation where $k_j - k_j^* = 1$, meaning that X_j and X_j^* differ by a single knot. We use this test statistic to select the number of knots and their location. In this way we obtain an iterative "general to specific" approach. At each step we calculate for all the knots in each column a Wald test with the null-hypothesis that a particular knot is not needed to form the true vector of factor loadings. We then remove the knot that has the smallest non-significant statistic among all the knots used to construct the loading matrix. The procedure is repeated until all selected knots have a statistically significant statistic. We start this iterative "general to specific" testing process with the unrestricted dynamic factor model.

2.5 Selecting knots: specific to general via Lagrange multiplier

The Lagrange multiplier test can also be used to test the hypothesis (10). It is based on the score vector with respect to parameters from the true data generation process in the jth column of Λ, that is

$$s(\bar{\lambda}_j) = \partial \ell(\bar{\lambda}_j) \,/\, \partial \bar{\lambda}_j,$$

where $\ell(\bar{\lambda}_j)$ is the loglikelihood function for a particular value of $\bar{\lambda}_j$ and where we adopt the notation of the previous section. This score vector can be evaluated analytically using Kalman filter methods as shown in Koopman and Shephard (1992). Since a spline in $\Lambda(X_j)$ is uniquely determined by vector $\bar{\lambda}_j$ and, similarly, a spline in $\Lambda(X_j^*)$ by $\bar{\lambda}_j^*$, the Lagrange multiplier test for null-hypothesis (7) is given by

$$s(\widehat{\bar{\lambda}}_j^*)' \widehat{V}_j^{*\,-1} s(\widehat{\bar{\lambda}}_j^*) \overset{a.}{\sim} \chi^2\left(K_j - K_j^*\right), \tag{12}$$

where $\widehat{\bar{\lambda}}_j^*$ is the maximum likelihood estimator of the (restricted) parameter vector $\bar{\lambda}_j^*$ and $\widehat{V}_j^*$ is a consistent estimator of the asymptotic variance of $\sqrt{nN}(\widehat{\bar{\lambda}}_j^* - \bar{\lambda}_j^*)$. In contrast to the

Wald test, here we need to estimate $\bar{\lambda}_j^*$ which is of a lower dimension than $\bar{\lambda}_j^\dagger$.

The iterative testing procedure for selecting the knots for the cubic spline function as described in the previous section can be carried out in a reverse way by means of the Lagrange multiplier test (12). We start with a highly restrictive specification, say we consider three knots for each column of the loading matrix; two of these knots are placed in the first and last rows of the factor loading column vectors. The parameters in this restrictive model are estimated by maximum likelihood. Based on the Lagrange multiplier test, a set of knots can be added to the jth column of Λ corresponding to positions where the score value is highest and most significant.

A practical method for selecting the knots within a "specific to general" approach is to consider each extension of the set of knots separately, that is, we have $k_j - k_j^* = 1$ for each row j of Λ. The single restriction with the most significant Lagrange multiplier test is then selected to be removed from the current set of restrictions. If not any restriction leads to a significant test statistic, the sequential knot selection procedure can be terminated. The test procedure is based on single or marginal hypotheses, not on joint hypotheses. Whether the "specific to general" approach is computationally less demanding than the "general to specific" approach is investigated as part of a simulation study in section 2.7.

2.6 Model selection via likelihood ratio

The likelihood ratio test can also be considered for selecting smoothness restrictions in loading matrix based on the hypothesis (10). For example, the test statistic can verify whether a reduction in the number of restrictions leads to a significant improvement of the loglikelihood value. The likelihood ratio test is given by

$$2 \times [\ell(\widehat{\bar{\lambda}}_j^\dagger) - \ell(\widehat{\bar{\lambda}}_j^*)] \overset{a.}{\sim} \chi^2\left(K_j - K_j^*\right), \tag{13}$$

where $\ell()$ is the loglikelihood function for a particular value of $\bar{\lambda}_j$ or $\bar{\lambda}_j^*$. We can adopt this statistic in both the "general to specific" and the "specific to general" approaches of knot selections. However, the procedure will become computationally more demanding since we need to estimate both $\bar{\lambda}_j^\dagger$ and $\bar{\lambda}_j^*$. The test statistic is not specific to the selection of smoothness restrictions within the context of a cubic spline function. It can be used for the testing of other restrictions in the dynamic factor model. In more general settings, the likelihood ratio test can be complemented with information criteria such as the well-known Akaike and Schwarz' Bayesian information criteria.

2.7 Monte Carlo evidence for knot selection procedures

To verify the success of our statistical procedures in identifying smoothness restrictions on the loadings, we carry out a Monte Carlo study. The design of the study is straightforward. We generate data from a dynamic factor model with a smooth loading matrix. The smoothness of the columns of the loading matrix is imposed by cubic spline functions. We are interested whether the true number of knots and the knot positions in the loading matrix can be detected from the generated data. This is a challenging task since cubic spline functions can become very similar even though different number of knots and different knot positions are used. For the Monte Carlo study we consider a dynamic factor model with $N = 17$ and $r = 3$ while the time series length is set for a small sample size, $n = 50$. The estimation requires r identification restrictions for each column of Λ, see the discussion at the beginning of section 2: we take rows 1, 9 and 17 equal to the subsequent rows of the identity matrix I_3. We simulate data from this dynamic factor model with smooth loadings based on 2 knots and on 6 knots (in addition to the the 3 restricted knots) for each column of Λ. In effect, we have either 6 or 18 knot coefficients that need to be estimated. The knots are evenly spaced over the columns of Λ, with the knot coefficient set to alternate between high $(2.0, 3.0, 4.0)$ and low $(-4.0, -3.0, -2.0)$ values. The factors f_t follow a vector autoregressive process with one lag order. The model is then formulated in the state space form (1) – (3) with $\mu_y = 0$, $H = I_N$, $Z = I_r$, $\mu_\alpha = 0$,

$$T = \begin{bmatrix} 0.9 & 0.1 & 0.05 \\ 0.1 & 0.75 & 0.1 \\ 0.05 & 0.1 & 0.5 \end{bmatrix}, \qquad Q = \begin{bmatrix} 0.5 & 0.2 & 0.2 \\ 0.2 & 0.5 & 0.2 \\ 0.2 & 0.2 & 0.5 \end{bmatrix}.$$

The generation of data mainly relies on drawing values for ε_t and η_t from the normal density. We carry out the knot selection procedure as detailed below for each generated time series. The Monte Carlo results are presented in Table 1 and are based on 100 replications.

We consider two knot selection procedures, one "general to specific" and one "specific to general" approach. First, the Wald procedure from section 2.4. Second, we employ a hybrid approach combining the Lagrange multiplier (LM) procedure from section 2.5 with the likelihood ratio (LR) approach of section 2.6. After the estimation of the parameters in a model with a given number of knots (starting with the model without any additional knot), we calculate the analytical score for each element in the factor loading matrix. Then, for each column we run a LR test on adding the knot that has the highest absolute score. We employ this hybrid approach to benefit from the accuracy of the LR test method and the computational speed of the LM approach. Since the LR test drives this selection procedure,

we refer to this approach as the LR test procedure. Finally, in all cases we use a 5% significance level for the test procedure.

Table 1: Simulation Study to Knot Accuracy

The table reports output from a simulation study to the accuracy of the knot selection procedure. For a given number of knots (# Knots DGP) from the factor loading matrix we simulate from a dynamic factor model, where we construct a smooth loading matrix using spline interpolation based on selected elements of the factor loadings matrix. We report the average difference (and standard deviation thereof, labelled *Sd*) between the estimated number of knots in our model, using both the Wald and LR knot selection procedure. In addition, we report the percentage of knots that is correctly estimated and the average time it takes to run the knot selection procedure.

Simulation Study					
# Knots		Difference		Perc	Avg
DGP	Est	Mean	Sd	Correct	Time
Wald Knot Selection Procedure					
6	8.98	2.98	2.98	66.8%	7.2
18	18.09	0.09	4.84	52.4%	8.9
LR-Score Knot Selection Procedure					
6	4.19	-1.81	1.96	79.3%	2.1
18	12.30	-5.70	5.55	52.7%	13.2

Table 1 reports the output from the simulation study. For both the LR and Wald procedure, the number of knots is estimated fairly accurately. With 6 knots in the model, the Wald procedure estimates on average 9.0 knots and the LR procedure 4.2 knots. Given the corresponding standard deviations of 3.0 and 2.0, respectively, these average values are well within a 95% confidence interval of 6 original knots. A similar result is found for the model with 18 knots. On average, the LR procedure produces a number of knots below the number of knots in the data generation process, and the Wald test leads to a higher number. It is likely due to the different set-ups of the two procedures: the Wald test procedure starts with the large model and removes knots, while the LR test procedure starts with the small model and adds knots.

We also present the percentage of occurrences in which the number of knots and its positions are correctly estimated, and the average time that it takes to reach the optimal model. For each replication, we compare the knots in the estimated loading matrix with those used in the "true" model to generate the data. We regard a knot as correctly detected if it is both a knot in the true and estimated loading matrix. For the other elements in Λ, we label an element as correct when it is not a knot in both the true and estimated loading matrix. For the model with 6 knots, the percentage of correctly placed knots is somewhat

higher for the LR procedure, 79% compared to 67%. In situations where the number of knots and the positions of the knots are correctly detected, we may expect a good fit but not necessarily. Neighbouring knots may lead to a similar or better fit and other shapes of the cubic spline function may be obtained by a smaller number of knots. This is also apparent for the model with 18 knots, where for both the Wald and LR procedure the percentage of correctly placed knots decreases.

We emphasize that our simulation results are based on a small sample of 100 observations over time. Given this small sample, we are satisfied by the simulation results reported in Table 1. The Wald test procedure requires overall less computing time because the likelihood needs to be optimized only once compared to three times for the LR test procedure. However, the LR test procedure requires less time for models with 6 knots because it starts with the model containing no knots and the Wald starts with the model having knots at all places in the factor loading matrix. In conclusion, the simulation study presents evidence that smoothness restrictions in the loadings matrix can be identified from data sufficiently accurate in small samples.

3 Empirical results

We have constructed a monthly time series panel of unsmoothed Fama-Bliss zero yields for U.S. treasuries of different maturities between 1970 and 2009; the details of the data set are provided in section 3.1. The estimation results for the unrestricted DFM are presented in sections 3.2. An important part for the smooth DFM is our knot-selection procedure based on the Wald and likelihood ratio test and the results are discussed in section 3.3 together with the estimation results of the selected model. We provide a comparison of our results with those for the dynamic Nelson-Siegel model in section 3.4 and the spline yield curve model in section 3.5. Finally, in section 3.6 we present the results of our forecasting study.

3.1 Data description

Our empirical study is based on a new data set of U.S. interest rates that is constructed in similar way as the data used in Diebold and Li (2006). A panel of monthly time series of zero yields from the CRSP unsmoothed Fama and Bliss (1987) forward rates is constructed. We refer to Diebold and Li (2006) for a detailed discussion of the method that is used for the creation of this data set. The resulting balanced panel data set consists of 17 maturities over the period from January 1970 up to December 2009, we have $N = 17$ and $n = 480$. The maturities we analyze are 3, 6, 9, 12, 15, 18, 21, 24, 30, 36, 48, 60, 72, 84, 96, 108

and 120 months. Similar but shorter datasets have been considered by Diebold, Rudebusch, and Aruoba (2006), Christensen, Diebold, and Rudebusch (2010) and Bowsher and Meeks (2008).

In Panel A of Figure 1 we present a three-dimensional plot of the data set. The data plot suggests the presence of an underlying factor structure. Although the yield series vary heavily over time for each of the maturities, a strong common pattern in the 17 series over time is apparent. For most months, the yield curve is an upward sloping function of time to maturity. The overall level of the yield curve is mostly downward trending over time in our sample period. These findings are supported by the time series plots in Panel B of Figure 1. We also observe that volatility tends to be lower for the yields of bonds with a longer time to maturity.

Table 2 provides summary statistics for our dataset. For each of the 17 time series we report mean, standard deviation, minimum, maximum and a selection of autocorrelation and partial autocorrelation coefficients. The summary statistics confirm that the yield curve tends to be upward sloping and that volatility is lower for rates on the long end of the yield curve. In addition, there is a very high persistence in the yields: the first order autocorrelation for all maturities is above 0.97 for each maturity. Even the twelfth autocorrelation coefficient can be as high as 0.85. The partial autocorrelation function suggests that autoregressive processes of limited lag order will fit the data well since only the first coefficient is significant for most maturities while the second lag coefficients are relatively small. (to preserve space we display a selection of coefficients). In Panel B of the Table 2 we present the sample correlations between yields of a selected number of maturities. The correlations are mostly above 0.9, in accordance with the strong common patterns in the movements of the different yields that we observe in Figure 1.

3.2 Estimation results for dynamic factor model

The models considered in this study belong to the class of dynamic factor models (1)–(3) and include a total of three latent factors, that is $r = 3$. Here we follow a growing number of studies that find three factors adequate for explaining most of the variation in the cross-section of yields; see, for example, Litterman and Scheinkman (1991), Bliss (1997) and Diebold and Li (2006). Other studies have recommended more factors, see the discussion in De Pooter (2007).

Our time series panel of U.S. interest rates for 17 maturities is represented by y_t and is modelled as in (1) with a 17×1 vector of constants μ_y, a full 17×3 loading matrix Λ, a 17×17 diagonal variance matrix H. For the identification of all parameters in the

Figure 1: Yield Curves from January 1970 through December 2009
In this figure we show the U.S. Treasury yields over the period 1970-2009. We examine monthly data, constructed using the unsmoothed Fama-Bliss method. The maturities we show are $3, 6, 9, 12, 15, 18, 21, 24, 30, 36, 48, 60, 72, 84, 96, 108$ and 120 months. Panel A presents a 3-dimensional plot, Panel B provides time-series plots for selected maturities.

(A) 3-Dimensional Term Structure Plot

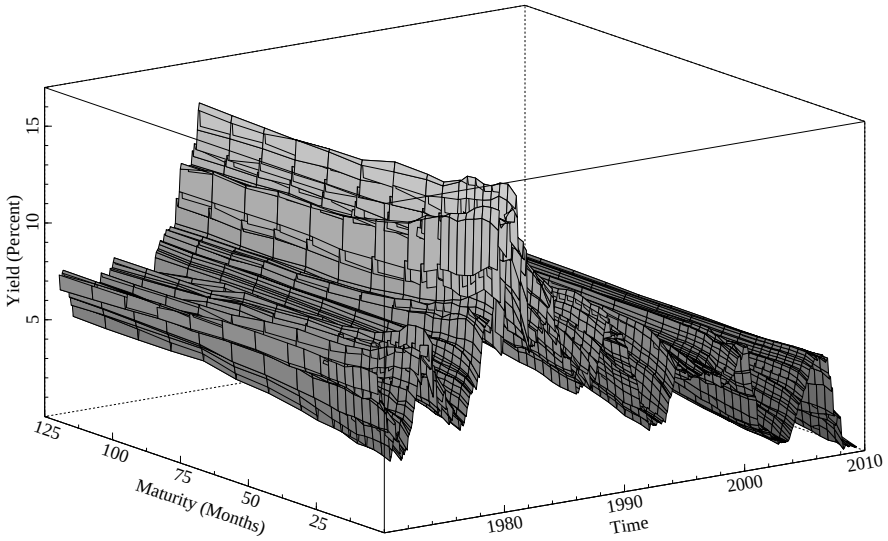

(B) Time-Series for Selected Maturities

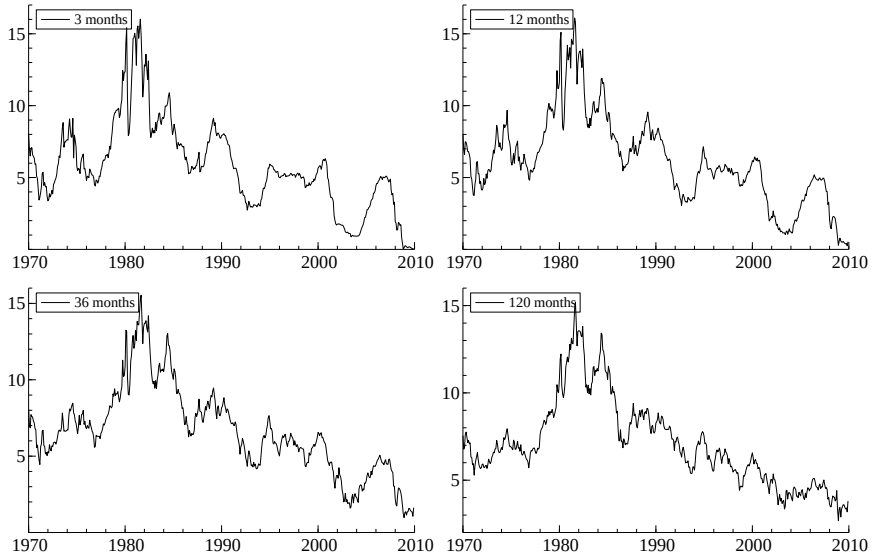

Table 2: Summary Statistics

The table reports summary statistics for U.S. Treasury yields over the period 1970-2009. We examine monthly data, constructed using the unsmoothed Fama-Bliss method. Maturity is measured in months. In Panel A we show for each maturity mean, standard deviation (*Sd*), minimum, maximum and two (1 month and 12 month) autocorrelation (*Acf*, $\hat{\rho}(1)$ and $\hat{\rho}(12)$ respectively) and two (2 month and 12 month) partial-autocorrelation (*Pacf*, $\hat{\alpha}(2)$ and $\hat{\alpha}(12)$) coefficients. In Panel B we show the correlation matrix for some selected maturities.

Panel A: Summary Statistics

					Acf		Pacf	
Maturity	Mean	Sd	Min	Max	$\hat{\rho}(1)$	$\hat{\rho}(12)$	$\hat{\alpha}(2)$	$\hat{\alpha}(12)$
3	5.77	3.07	0.04	16.02	0.98	0.75	-0.11	-0.06
6	5.97	3.09	0.15	16.48	0.98	0.76	-0.13	-0.11
9	6.08	3.09	0.19	16.39	0.98	0.77	-0.14	-0.12
12	6.17	3.05	0.25	16.10	0.98	0.78	-0.15	-0.13
15	6.25	3.03	0.38	16.06	0.98	0.78	-0.15	-0.13
18	6.32	3.01	0.44	16.22	0.98	0.79	-0.15	-0.14
21	6.39	2.99	0.53	16.17	0.98	0.80	-0.14	-0.15
24	6.42	2.94	0.53	15.81	0.98	0.80	-0.16	-0.14
30	6.51	2.88	0.82	15.43	0.98	0.81	-0.13	-0.13
36	6.60	2.83	0.98	15.54	0.98	0.81	-0.13	-0.11
48	6.76	2.75	1.02	15.60	0.98	0.82	-0.11	-0.12
60	6.85	2.67	1.56	15.13	0.99	0.83	-0.10	-0.12
72	6.96	2.64	1.52	15.11	0.99	0.84	-0.11	-0.12
84	7.03	2.57	2.18	15.02	0.99	0.84	-0.12	-0.11
96	7.07	2.53	2.11	15.05	0.99	0.85	-0.12	-0.12
108	7.10	2.52	2.15	15.11	0.99	0.85	-0.14	-0.14
120	7.07	2.46	2.68	15.19	0.99	0.84	-0.12	-0.13

Panel B: Correlation Matrix for Selected Maturities

Maturity	3	12	36	60	120
3	1.00	0.99	0.96	0.93	0.90
12		1.00	0.98	0.96	0.93
36			1.00	1.00	0.98
60				1.00	0.99
120					1.00

DFM and to keep the VAR(k) coefficient matrices unrestricted, we restrict the three rows corresponding to maturities of 1 (first row), 30 (ninth row) and 120 months (last row) in Λ. In particular, this set of three rows is set equal to

$$\lambda_{1,\cdot} = (1, 1, 0), \qquad \lambda_{9,\cdot} = (1, \frac{1}{2}, 1), \qquad \lambda_{17,\cdot} = (1, 0, 0). \tag{14}$$

These restrictions facilitate comparison with the factors of the Nelson-Siegel yield curve in section 3.4 to some extent while the set of restrictions is not singular. We have noticed that the estimation results are not qualitatively different when we consider another set of restrictions (for example, the rows of the identity matrix I_3) since we can rotate the factors such that another set of restrictions is implied. The dynamic specification for the three factors in f_t are modelled jointly by a vector autoregressive process of lag order 1 and is given by

$$f_{t+1} = \Phi f_t + \eta_t, \qquad \eta_t \sim \text{NID}(0, Q), \qquad t = 1, \ldots, n, \tag{15}$$

which can be expressed as in (3) with $\mu_\alpha = 0$, $T = \Phi$, $R = I$ and $\alpha_t = f_t$. We denote this model by VAR(1). In our empirical study, we consider the VAR(1) specification for the factor process in all model specifications. This choice is the same as in related studies such as Diebold, Rudebusch, and Aruoba (2006); the exception is Bowsher and Meeks (2008) where a cointegrated VAR system with multiple lags is considered for the factors.

The maximum likelihood estimates of the factor loadings are presented in the three columns of Panel A of Table 3. It shows that the loadings associated with the first factor are very close to unity and therefore we can interpret the first factor as the level. The loading estimates for the second factor are smoothly descending from one to zero for interest rates of ascending maturity. This is the typical Nelson and Siegel (1987) shape for their second factor which they associate with the slope of the yield curve. Their third factor is designed as the curvature of the yield curve with the associated loading pattern given by an asymmetric, reverse U-shape. Our loading estimates for the third factor also admit to this pattern and therefore we can interpret the third factor in f_t as the curvature of the yield curve at time t. How close our estimated loadings are to the Nelson-Siegel loadings is discussed in section 3.4. In case of the DFM, the loading restrictions in (14) have facilitated the level-slope-curvature (LSC) interpretation of the three factors. When other loading restrictions were considered, the estimation results are not different since appropriate factor rotations can be carried out to obtain the same loadings as presented in Table 3.

Table 3: Selection of SDFM Specifications

This table shows the factor loading matrix for the DFM and SDFM specifications. We select the knots in the SDFM using both the iterative LR and Wald test procedures. Numbers in italics indicate that no knot is estimated at the location, but the value is interpolated using the spline for the corresponding column. Asterisks (∗/∗∗) indicate whether the probability of the null (the knot is not necessary) is lower than 5%/1%.

Factor Loading Matrix of DFM and SDFM									
	Loadings DFM			Loadings SDFM, Wald			Loadings SDFM, LR		
Maturity	Factor 1	Factor 2	Factor 3	Factor 1	Factor 2	Factor 3	Factor 1	Factor 2	Factor 3
3	1.000	1.000	0.000	1.000**	1.000**	0.000**	1.000**	1.000**	0.000**
6	1.009	0.973	0.253	*0.999*	*0.964*	*0.241*	*1.013*	*0.956*	*0.213*
9	1.013	0.917	0.439	*0.999*	*0.917*	0.469**	1.016**	*0.905*	*0.423*
12	1.005	0.850	0.645	1.001*	0.848**	*0.668*	1.007**	0.841**	0.628**
15	1.006	0.764	0.829	1.004*	0.761**	0.821**	*1.007*	*0.763*	0.807**
18	1.012	0.700	0.890	*1.008*	0.700**	*0.913*	*1.015*	0.691*	*0.889*
21	1.017	0.645	0.918	*1.010*	0.647**	*0.960*	1.017**	0.643*	*0.912*
24	1.008	0.595	0.946	1.007**	0.594**	*0.981*	*1.009*	0.592**	0.942**
30	1.000	0.500	1.000	1.000**	0.500**	1.000**	1.000**	0.500**	1.000**
36	1.002	0.424	0.957	0.999**	0.426**	1.000**	1.001**	0.426**	*0.965*
48	1.004	0.301	0.852	*0.999*	0.304**	0.879**	*1.000*	0.304**	*0.856*
60	0.997	0.212	0.729	*1.000*	0.211**	0.741**	0.997**	0.215**	0.742**
72	1.003	0.138	0.636	*1.000*	0.140**	0.661**	*0.995*	*0.146*	0.649**
84	0.997	0.091	0.470	*1.000*	0.088**	0.473**	*0.995*	*0.088*	*0.490*
96	1.002	0.039	0.316	*1.000*	0.040**	0.329**	*0.996*	0.045**	0.335**
108	1.007	0.014	0.192	*1.000*	*0.012*	0.213**	*0.998*	*0.018*	0.226**
120	1.000	0.000	0.000	1.000**	0.000**	0.000**	1.000**	0.000**	0.000**

Table 4: Estimated Transition and Variance Matrices
In these two tables we present the eigenvalues of the estimated transition matrices for the DFM and SDFM model, obtained using the iterative LR test procedure. The column with heading 'real' contains the real part of the eigenvalues and the column with heading 'img.' contains the imaginary parts. Eigenvalues are sorted in ascending order. In Panel A we report results for the DFM model, in Panel B for the SDFM model.

Panel A: Transition and Variance Matrix for DFM									
	Transition Matrix			Eigenvalues			Variance Matrix		
	$\alpha_{1,t-1}$	$\alpha_{2,t-1}$	$\alpha_{3,t-1}$	#	real	img.	$\alpha_{1,t}$	$\alpha_{2,t}$	$\alpha_{3,t}$
$\alpha_{1,t}$	0.995	0.018	-0.063	1	0.929	-0.004	0.112	0.018	0.016
$\alpha_{2,t}$	-0.009	0.963	0.140	2	0.929	0.000	0.018	0.150	-0.012
$\alpha_{3,t}$	0.009	-0.006	0.891	3	0.991	0.004	0.016	-0.012	0.026

Panel B: Transition and Variance Matrix for SDFM									
	Transition Matrix			Eigenvalues			Variance Matrix		
	$\alpha_{1,t-1}$	$\alpha_{2,t-1}$	$\alpha_{3,t-1}$	#	real	img.	$\alpha_{1,t}$	$\alpha_{2,t}$	$\alpha_{3,t}$
$\alpha_{1,t}$	0.995	0.017	-0.063	1	0.929	-0.004	0.112	0.018	0.015
$\alpha_{2,t}$	-0.009	0.963	0.141	2	0.929	0.000	0.018	0.154	-0.012
$\alpha_{3,t}$	0.008	-0.006	0.891	3	0.991	0.004	0.015	-0.012	0.026

The autoregressive coefficient matrix Φ and the variance matrix Q in (15) are estimated jointly with μ_y, Λ and H in (1) by the method of maximum likelihood. The estimates for Φ and Q are presented in Panel A of Table 4. The leading diagonal of the estimated Φ contains values between 0.995 and 0.89 while the off-diagonal elements are all smaller than 0.15 in absolute value. It indicates that the factors are highly persistent over time. To provide a further insight in the dynamic persistence of the factors, we report the eigenvalues of the estimated autoregression matrix Φ in Table 4. The two eigenvalues of 0.99 and 0.93 are close to one and have a small imaginary part while one eigenvalue of 0.93 has no imaginary component. We can therefore view the factors as a weighted sum of one persistent autoregressive process and two persistent (weakly) cyclical processes.

3.3 Estimation results for smooth loadings

Next we analyze the results that we obtain by applying the method of section 2.4 for finding a suitable set of smoothness restrictions for the factor loadings of the DFM model. To ensure that the loadings in the SDFM are identified, we impose the same loading restrictions

(14) as for the DFM. Although the estimation results for the DFM are not sensitive to different restriction choices, once we start to interpolate factor loadings, the positions of the restrictions can affect the optimal smoothing conditions. We let the restrictions (14) correspond to the 3, 30, and 120 months of maturities. The interpolating cubic spline framework requires knot positions at the begin- and end-points (3 and 120 months) while the knot position of 30 months remains fixed during the selection procedure. However, the selection procedure can be repeated after moving the knot of 30 months to another time to maturity. After some experimentation, we have verified that our main results are not sensitive to moving this knot for 30 months to neighbouring times to maturity.

In the final six columns of Table 3 we present the estimated loadings that are based on knot positions obtained from the knot selection procedures of sections 2.4, 2.5 and 2.6. At the start of the procedure, we consider the unrestricted DFM for which 12 out of 42 loading coefficients (or knots) are significant at the 5% significance level (results omitted for brevity, but available upon request). This suggests that the number of parameters can be reduced without affecting the fit significantly. However, the test statistics are strongly correlated and removing one knot will change the test statistics for the neighbouring knots. We therefore proceed by sequentially removing the knot with the lowest Wald-statistic and re-estimating the model after each step, see section 2.4. This "general to specific" procedure is terminated when all test statistics for the remaining knots are significant at the 5% significance level. The middle three columns show the smooth dynamic factor model obtained from this procedure. In addition, we consider a specific to general selection procedure that is based on a hybrid approach of merging the Lagrange multiplier procedure of section 2.5 and likelihood ratio statistic procedure of section 2.6 which starts with the most parsimonious model based on knot values implied by the loading restrictions (14). By subsequently adding a knot at positions where the restriction is rejected most strongly, we obtain the hybrid "specific to general" procedure as also described in section 2.7. We refer to this approach as the LR test procedure.

To let a cubic spline fit a certain shape, the distribution of the knots is generally more important than the exact location of the knots. First, we look at the knot selection procedure based on the Wald statistics. We find that the selection procedure is successful in fitting the first column of factor loadings, as the fourth column of Table 3 is close to the first column from the DFM. The original set of 14 unrestricted loading parameters is reduced to four remaining knot parameters. Given that all original estimates are close to unity, this result may not be surprising. Overall, we reduced the number of parameters in the loading matrix Λ by 18, a reduction of 43 percent. The resulting values for the loadings are close to those of the DFM in Panel A. The results for our second LR selection procedure are presented in

the three columns of Panel C. In this procedure we add a knot at the position where the restriction is rejected most strongly. When all remaining restrictions are not rejected, the selection procedure is completed. At the final stage we estimate all knots and compute the associating standard errors and these results are presented in Panel C. The results in for the two knot selection procedures are very close to each other. However, the LR procedure has reduced the number of parameters in Λ by 22, a reduction of 52 percent. The resulting model is therefore more parsimonious than the one obtained from the Wald procedure. This result confirms our findings from the simulation study in section 2.7.

In Panel A of Figure 2 we graphically present the factor loading estimates (dots) of the DFM together with cubic spline estimates for the factor loadings of the SDFM obtained from the LR procedure (solid line). For all three factors, the estimated factor loading patterns are smooth. Those for the DFM and SDFM are not distinguishable from each other in the graph. We therefore have shown that we can achieve almost identical loadings using a much smaller set of parameters. It confirms our prior believe that the true factor loadings are subject to smoothness restrictions.

Given that the factor loadings for the DFM and SDFM specifications are very similar, we do not expect that the dynamic properties of the factors as modelled by (15) are estimated very differently for the two models. In Panel B of Table 4 we present the estimates of Φ, including its eigenvalues, and Q for the SDFM, as obtained from the LR procedure, and we conclude that these estimates are very close to those presented in Panel A for the DFM. To complete the presentation of the estimation results for the SDFM, we graphically present in Figure 3 the estimates of α_y in Panel A and of the diagonal of H in Panel B. The intercept pattern is upward sloping and concave in a similar way as the sample means which are reported in Table 2. The estimated measurement error variance pattern is different from the decreasing pattern of the sample standard deviations which are presented in Table 2. The short term interest rates contain more measurement noise compared to interest rates for more than one year to maturity irrespective of time to maturity. The measurement noise decreases for longer maturities within the range of one year to maturity. The measurement noise increases somewhat for the longest times to maturity. To present further evidence that the DFM and SDFM model specifications produce qualitatively the same in-sample results, we present in Panel A of Figure 4 the three factor estimates for both model specifications. The factor estimates are obtained from a signal extraction procedure that is described in section 2.1. In all three plots, the factor estimates are indistinguishable from each other.

In Table 5 we report a selection of statistics for the unrestricted and smooth dynamic factor models. It enables comparisons of in-sample fit, accounting for the number of parameters that are estimated. The DFM contains 91 parameters and its maximized loglikelihood

Figure 2: Estimated Factor Loadings for DFM and SDFM Model

This figure shows the estimated factor loadings as functions of time to maturity for the optimal SDFM model, obtained using the iterative LR test procedure. For ease of comparison we also show the maximum likelihood estimates of the loadings in the DFM model. The loadings are restricted with the rows of the identity matrix at the 3 months, 30 months and 120 months maturities. Panel (A) plots the factor loadings as estimated for the DFM and SDFM, together with those of the Nelson-Siegel model for reference. Panel (B) shows the factor loadings from Panel (A) rotated towards the factor loadings of the Nelson-Siegel model.

(A) Factor Loadings of DFM, SDFM and NS

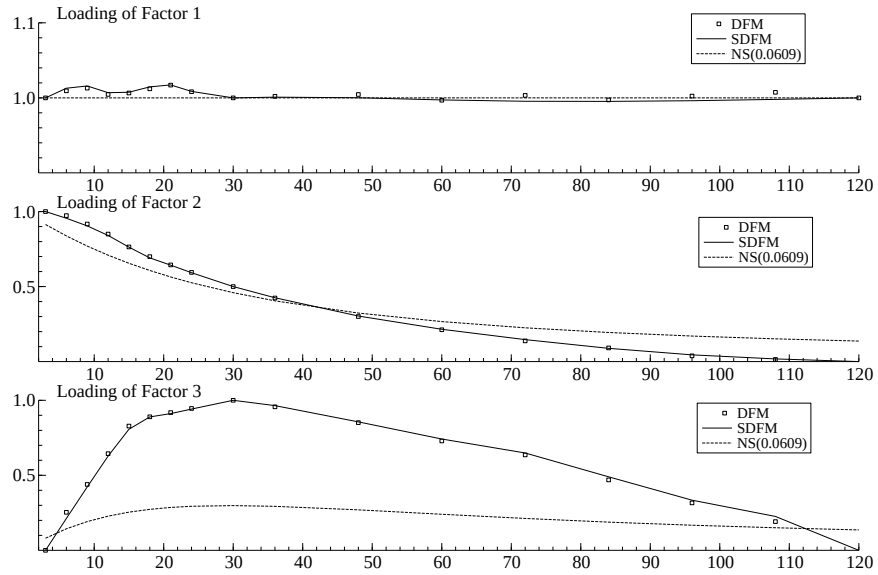

(B) DFM and SDFM Loadings rotated to NS

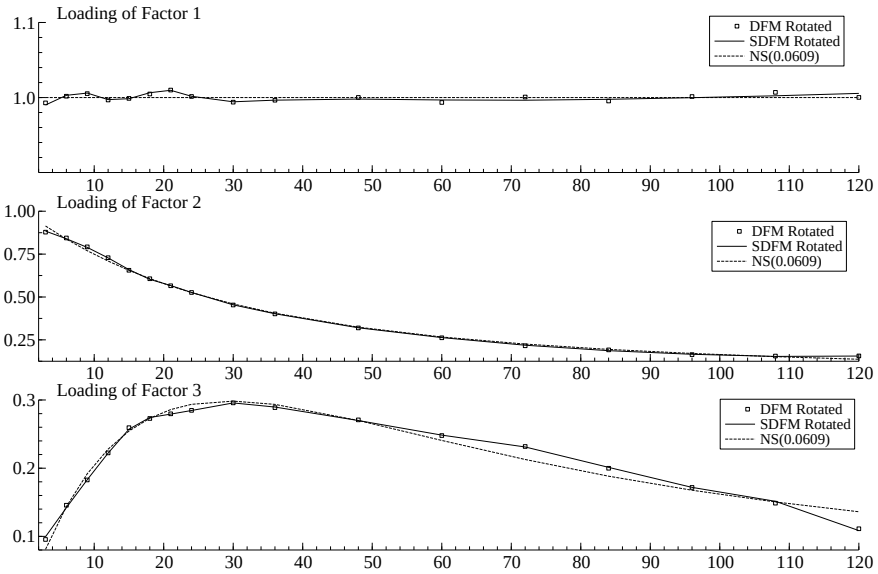

Figure 3: Intercept and Measurement Error Variance

In this figure we show the intercept and measurement error variance as functions of time to maturity from the SDFM model, obtained using the iterative LR test procedure. For ease of comparison we also show these for the DFM model.

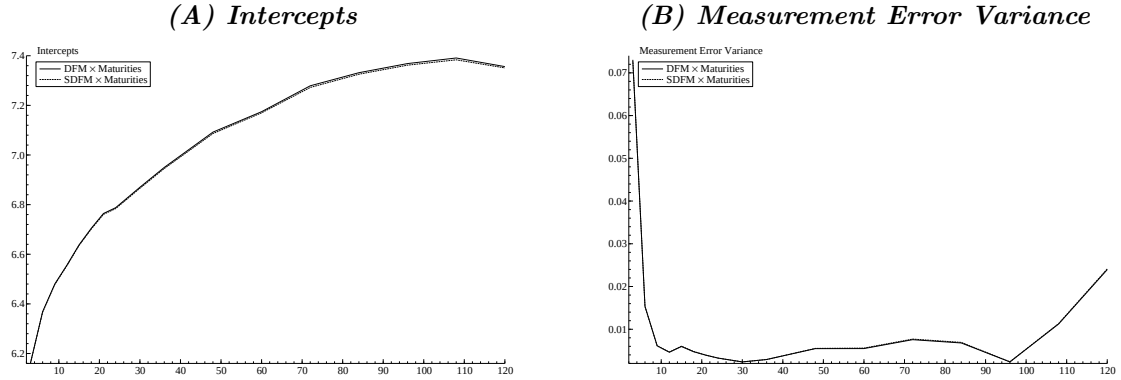

Figure 4: Smoothed Factors for DFM and SDFM Model

In this figure we show the smoothed time series of the latent factors for the SDFM model, obtained using the iterative LR test procedure. For ease of comparison we also show these for the DFM model in the same figures, and of the Nelson-Siegel model in the right figures.

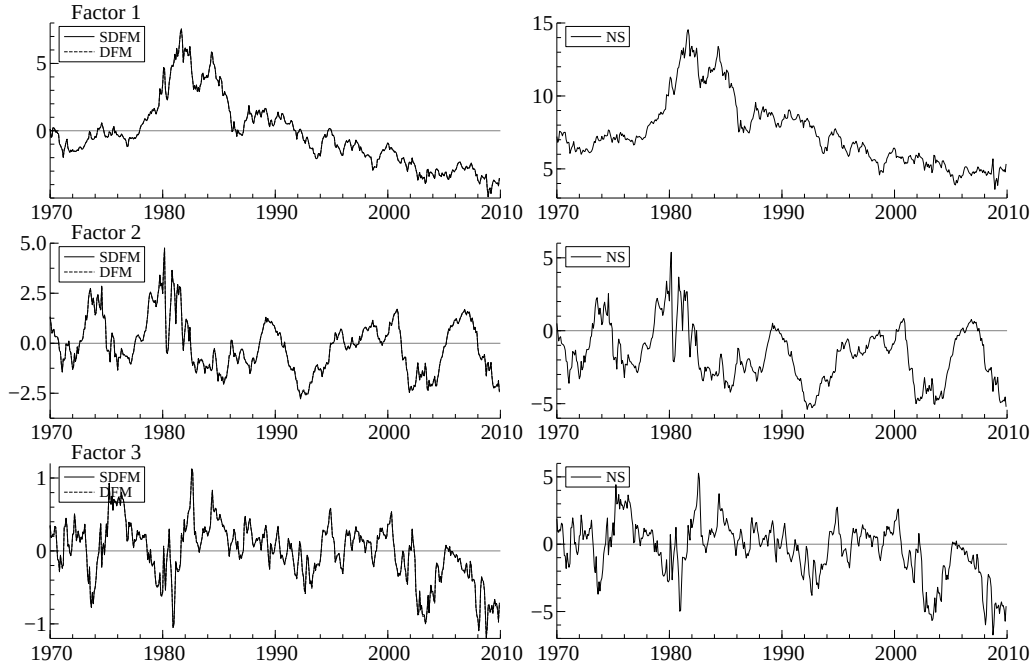

Table 5: Comparison of Models based on Likelihood

This table presents the various measures useful for comparing the in-sample fit of the considered models. The column Loglikelihood provides the loglikelihood, LR the likelihood-ratio and #Pars the number of parameters. The last two columns present output from two information criteria: the Akaike Information Criterion (AIC) and Schwarz Information Criterion (SIC). We show the measures for the DFM, SDFM using both the Wald and LR knot selection procedure, Nelson-Siegel and Functional Signal plus Noise (FSN) models.

Model Comparison					
Model	Loglikelihood	LR	#Pars	AIC	SIC
DFM	6,135.2		91	-12,088.4	-11,708.6
SDFM(Wald)	6,085.0	100.4	73	-12,024.0	-11,719.3
SDFM(LR)	6,110.4	49.6	69	-12,082.8	-11,794.8
NS	5,658.6	953.2	36	-11,245.2	-11,094.9
FSN	5,093.5	2,083.4	35	-10,117.0	-9,970.9

value is given by 6135.2. After running our knot selection procedures, we obtain far less parameters. Using the Wald procedure we obtain a model with 73 parameters while using the likelihood ratio based approach the model consists of 69 parameters. In both cases the loglikelihood is maximized at roughly the same value, 6085.0 and 6110.4, respectively. A likelihood ratio test for the joint significance of the 18 or 22 restrictions rejects the null hypothesis in both cases. However, the Schwarz information criterion, taking the large number of observations into account for the model selection, favors our smooth factor models over the unrestricted version. Since the SDFM based on the hybrid likelihood ratio selection procedure has a similar likelihood but with a smaller number of parameters, we recommend this approach. We should note that the two resulting SDFMs are not nested since the weight matrices are different for both models; both SDFMs are however nested with the DFM.

The knot selection procedures for obtaining the SDFM specifications require the estimation of parameters in many intermediate SDFM specifications. Many of these model specifications contain over 90 parameters which are estimated by the method of maximum likelihood. This task may appear computationally intensive from the outset. However, the computationally efficient methods discussed in section 2.1 make our approach computationally feasible and a matter of routine, even for higher dimensional models.

3.4 Comparisons with the Nelson-Siegel yield curve

In an important contribution Nelson and Siegel (1987) have shown that the term structure can surprisingly well be fitted by a linear combination of three smooth functions. The Nelson-Siegel yield curve is then given by

$$f^L + \lambda_S(\tau) \cdot f^S + \lambda_C(\tau) \cdot f^C, \tag{16}$$

where f^L, f^S and f^C are treated as the level, slope and curvature (LSC) factors, respectively, and the corresponding factor weights for slope and curvature are functions of time to maturity τ, that is

$$\lambda_S(\tau) = \frac{1 - e^{-\lambda\tau}}{\lambda\tau}, \qquad \lambda_C(\tau) = \frac{1 - e^{-\lambda\tau}}{\lambda\tau} - e^{-\lambda\tau}, \tag{17}$$

with unknown coefficient $\lambda > 0$. The interpretation of the LSC factors is obtained as follows. The factor f^L is by construction the overall *level* of the yield curve. The factor f^S is associated with the *slope* of the yield curve since its loading $\lambda^S(\tau)$ is high for a short maturity τ and low for a long maturity. The loadings $\lambda_C(\tau)$ is an inverted U-shaped function of τ and therefore f^C can be interpreted as the *curvature* of the yield. The decomposition of the yield curve into these LSC factors has also been highlighted by Litterman and Scheinkman (1991).

The LSC factors f^L, f^S, f^C and the coefficient λ, are treated as parameters which can be estimated at each time t by a least squares method based on the nonlinear regression model

$$y_{it} = f^L + \lambda_S(\tau_i) \cdot f^S + \lambda_C(\tau_i) \cdot f^C + u_{it}, \qquad i = 1, \ldots, N,$$

where y_{it} is the interest rate at time t for time to maturity τ_i and where u_{it} is a noise term with zero mean and possibly different variances for different times to maturity τ_i, for $i = 1, \ldots, N$.

The Nelson-Siegel yield curve can also be incorporated in a dynamic factor model by placing the LSC factors into the vector $\tilde{f}_t$ and to let them evolve as a time-varying process. We obtain

$$y_t = \mu_y + \Lambda_{ns}\tilde{f}_t + \varepsilon_t, \qquad \varepsilon_t \sim NID(0, H), \tag{18}$$

where the 3×1 vector $\tilde{f}_t$ represents the LSC factors and is modelled as a VAR(1) process as in (15) while H is a diagonal variance matrix. The ith row of the loading matrix Λ_{ns} is given by $[1\,,\, \lambda_S(\tau_i)\,,\, \lambda_C(\tau_i)]$. The resulting dynamic Nelson-Siegel (DNS) model can also be regarded as a smooth dynamic factor model in which the smoothness in the loading matrix is determined by the functional form (17) and parameter λ. The loading matrix Λ_{ns} depends

on a single parameter λ and is therefore more restrictive than the SDFM. The DNS model is proposed by Diebold, Rudebusch, and Aruoba (2006). Their specification is slightly different as they set μ_y in (18) to zero and include an intercept in the specification (15) for $\tilde{f}_t$.

The DNS model can clearly also be represented in the state space form (1)–(3) and we can estimate the parameters of the model as described in section 2.1. We follow the practice of Diebold, Rudebusch, and Aruoba (2006) by setting λ fixed at 0.0609. The remaining parameters in the DNS are estimated for the data set of section 3.1. In Panel A of Figure 2 the DNS loadings are presented as a dotted line and can be compared with those for the DFM and SDFM. Although the shapes of the loading patterns are similar, the loading values from the DNS model are clearly different. However, we can rotate the factors in the DFM and SDFM in such a way that the loadings become very close to those of the Nelson-Siegel loadings. The result of the DFM and SDFM loading rotations are presented in Panel B and we can conclude that the DFM and SDFM can approximate the LSC factors from the DNS model with a high degree of precision. Whether the results for in-sample and out-of-sample fit are different for the different models will be discussed next.

The differences between the extracted factors from the SDFM (not rotated to DNS) and from the DNS model can be detected when comparing the plots in on the left to those on the right of Figure 4. The level and scale of the SDFM and DNS factors are different which is due to the different estimates of μ_y and factor loadings themselves. However, the paths of the factors through time for the two different models are very similar. Finally, Table 5 also reports the optimized likelihood and information criteria for the Nelson-Siegel model. The model produces a far lower loglikelihood value such that it has a far higher LR compared to the smooth factor models. The information criteria take the far lower number of parameters into account (36 in the Nelson-Siegel model compared to 91 in the DFM), but still favor the dynamic factor models over the Nelson-Siegel model. A possible explanation for why the factors and loadings appear similar in the models but result in very different likelihood values, is the high precision with which the model is estimated. In additional results, we show that the confidence intervals around the estimated loadings are very narrow. It implies that small perturbations in the maximum likelihood estimates will cause large changes in the loglikelihood value.

3.5 Comparisons with the spline yield curve

A recent alternative for the Nelson-Siegel yield curve is proposed by Bowsher and Meeks (2008) who adopt the cubic spline function for describing the smooth term structure of interest rates. They have labelled their approach as the functional signal plus noise (FSN)

model. The modelling of the smooth signal vector Λf_t directly in terms of a cubic spline function is discussed in section 2.3. The spline yield curve is based on the observation equation given by

$$y_t = W'\bar{f}_t + \varepsilon_t, \qquad \bar{f}_t = Z\alpha_t, \tag{19}$$

where the spline weight matrix W and the coefficient vector $\bar{f}_t$ are defined in section 2.3, the time-varying specification $\bar{f}_t = Z\alpha_t$ replaces (2) and the dynamic specification for α_t is given by (3). To facilitate comparisons with DFM, SDFM and DNS in the context of interest rate series for different times to maturity, we consider three factors in $\bar{f}_t$. For the construction of the spline through times of maturity and the corresponding spline weights in W, we place knots at the positions 3, 30 and 120 months to maturity. Hence we can interpret the three factors in $\bar{f}_t$ as factors representing interest rates associated with the short, medium and long times to maturity. This interpretation of $\bar{f}_t$ deviates from the LSC interpretation of the Nelson-Siegel factors. Given the construction of the cubic spline weights in which the columns of W at the knot positions equal the identity matrix, we can provide the three factors of the FSN spline yield coefficients in $\bar{f}_t$ with a LSC interpretation. By pre-multiplying W with the matrix $B = [\lambda'_{1,\cdot}, \lambda'_{9,\cdot}, \lambda'_{17,\cdot}]$ where $\lambda_{j,\cdot}$ is defined in (14) for $j = 1, 9, 17$, we obtain the loading matrix $W_{lsc} = BW$ which leads to the LSC interpretation of the factors in $\bar{f}_t$ that determine the spline yield curve $W'_{lsc}\bar{f}_t$. The interpretation follows immediately since the jth column of W equals $\lambda_{j,\cdot}$ for $j = 1, 9, 17$.

Table 5 also reports the optimized likelihood and information criteria for the FSN model. The number of parameters is further reduced to 35, as W contains no parameters but is solely determined by the positions of the knots. Similar to the Nelson-Siegel model, the FSN model produces a loglikelihood that is far lower than the smooth factor models. The information criteria also do not favor this model. When compared to the Nelson-Siegel model, the FSN likelihood is also lower.

3.6 Forecasting results

To investigate the out-of-sample fit for the DFM, SDFM, DNS and FSN specifications for our panel time series of U.S. interest rates, we carry out a forecasting exercise. We forecast the full yield curve (the interest rates for 17 times to maturity) up to 24 months ahead. We forecast the yield curve for the months from January 1994 up to December 2009. To obtain the 24 month ahead forecast of the yield curve for January 1994, we estimate the parameters in the four different models using the observations of the time series panel from January 1970 up to January 1992. The 23 month ahead forecast for January 1994 and the 24 month ahead forecast for February 1994 are obtained by estimating the parameters in

the four different models based on the data from January 1970 up to February 1992. In this way we compute the forecasts, and the corresponding forecast errors, for $h = 1, 6, 12, 18, 24$ months ahead. We record the forecast errors for each forecast horizon, for each maturity and for each model. Then we compute the root mean square forecast error (RMSFE) for all these cases. The results of this extensive forecasting study are partially reported in Table 6. The re-estimation of the parameters in the different models is an extensive numerical task but it remains feasible when using the methods discussed in section 2.1. For simplicity, we fix the number of knots for different sample periods and we also keep the knot positions as obtained from the knot selection procedure based on the LR test. The selection is based on the full sample. Alternative strategies where we, for example, yearly repeat the knot selection procedure have yielded similar forecasting results.

In Panel A of Table 6 we report the forecasting results for the expanding window by means of the RMSFEs for the times to maturity 3, 12, 36, 60, 120 months. The one-month ahead forecasts for the 3-month interest rate is clearly the lowest for the forecasts produced by the SDFM while for the other times to maturity the RMSFE are more or less equal for all models. The multiple-months ahead forecasts produced by the SDFM have RMSFEs that are comparable to those from the DFM. The smoothing restrictions imposed by the DNS appear to lead to somewhat higher RMSFEs throughout except for one-year interest rates although in this case the differences are small. The FSN model provides RMSFEs that are particularly favorably in intermediate maturities at the short horizon. In Panel B we examine the robustness of the forecasting improvement. We show the RMSFEs for the periods 1994-1998, 1999-2003 and 2004-2009. We can observe some variation over these periods, the SDFM forecast precision are comparable to, or even better than, those of the Nelson-Siegel model. In the first two subsamples the SDFM produces the lowest RMSFEs, while in the last subsample the FSN model performs remarkably well but the differences are small in all subsamples. We can conclude that the smoothing restrictions imposed on the DFM do not affect the precision of the forecasts and often achieve the highest precision. These results are of course relative to our newly constructed data set of U.S. interest rates.

Table 6: Forecasting Performance of Factor Models

In these tables we present the forecasting performance of the various models. We show the root mean square forecast error (RMSFE) for the SDFM with knots from the LR procedure, the general DFM, Nelson-Siegel in SSF (NS-SSF) and and Functional Signal plus Noise (FSN) models. In Panel A we show results for the 1994-2009 sample, in Panel B for three different subperiods (1994-1998, 1999-2003 and 2004-2009). For each model the RMSFE is reported for 3 month, 1, 3, 5 and 10 year maturities, and h=1, 6, 12, 18 and 24-month ahead forecasts.

Panel A: Forecasting Performance 1994-2009					
	3 month	1 year	3 year	5 year	10 year
SDFM					
h=1	**0.314**	0.274	0.321	0.314	0.304
h=6	**0.956**	1.009	0.959	**0.869**	**0.678**
h=12	1.615	1.628	1.426	**1.243**	**0.939**
h=18	2.096	2.068	**1.758**	**1.507**	**1.101**
h=24	2.438	**2.396**	**2.026**	**1.734**	**1.275**
DFM					
h=1	0.328	0.273	0.320	0.315	0.300
h=6	0.959	1.008	0.958	0.871	0.679
h=12	**1.614**	1.626	**1.426**	1.246	0.943
h=18	**2.094**	2.067	1.759	1.512	1.110
h=24	**2.435**	2.397	2.028	1.741	1.288
NS-SSF					
h=1	0.347	0.271	0.321	0.319	**0.293**
h=6	0.998	1.004	0.965	0.878	0.696
h=12	1.671	1.622	1.440	1.259	0.981
h=18	2.166	**2.064**	1.781	1.532	1.169
h=24	2.526	2.400	2.061	1.772	1.367
FSN					
h=1	0.379	**0.265**	**0.316**	**0.310**	0.295
h=6	0.969	**0.989**	**0.953**	0.886	0.721
h=12	1.665	**1.614**	1.437	1.281	1.010
h=18	2.183	2.073	1.803	1.581	1.205
h=24	2.553	2.414	2.091	1.827	1.393

Panel B: Forecasting Performance for Subperiods															
	Forecasting Performance 1994-1998					Forecasting Performance 1999-2003					Forecasting Performance 2004-2009				
	3 month	1 year	3 year	5 year	10 year	3 month	1 year	3 year	5 year	10 year	3 month	1 year	3 year	5 year	10 year
SDFM															
h=1	**0.153**	0.252	**0.279**	0.290	0.311	**0.280**	0.300	0.352	0.343	0.298	0.422	0.268	0.326	0.307	0.303
h=6	0.483	0.715	**0.783**	**0.798**	0.771	1.112	1.216	1.084	0.949	**0.673**	1.101	1.028	0.979	0.855	**0.595**
h=12	0.758	**0.940**	**1.013**	**1.035**	**1.005**	1.932	2.020	**1.666**	**1.399**	**0.974**	1.836	1.711	1.502	1.262	**0.848**
h=18	**0.850**	**0.949**	**0.999**	**1.032**	**0.999**	2.493	**2.548**	**2.056**	**1.703**	**1.186**	2.437	2.289	1.972	1.658	**1.108**
h=24	**0.938**	**0.968**	**0.961**	**0.992**	**0.937**	**2.877**	**2.931**	**2.397**	**2.010**	**1.469**	2.866	2.714	2.321	1.957	**1.345**
DFM															
h=1	0.154	0.252	0.279	0.294	0.303	0.305	0.299	0.350	0.343	**0.297**	0.435	0.267	0.326	0.309	0.300
h=6	**0.477**	0.715	0.784	0.801	0.770	1.118	1.214	1.083	0.950	0.674	1.105	1.027	0.978	0.858	0.596
h=12	**0.755**	0.941	1.015	1.039	1.007	**1.931**	2.019	1.666	1.403	0.980	1.834	1.708	1.499	1.264	0.852
h=18	0.850	0.951	1.003	1.039	1.007	**2.493**	2.550	2.060	1.711	1.200	2.431	2.286	1.969	1.660	1.114
h=24	0.942	0.975	0.968	1.004	0.952	2.877	2.935	2.402	2.021	1.486	2.860	2.712	2.320	1.960	1.352
NS-SSF															
h=1	0.185	**0.244**	0.279	**0.289**	**0.275**	0.289	0.301	0.354	0.353	0.309	0.472	0.266	0.325	0.313	**0.293**
h=6	0.559	**0.710**	0.787	0.799	**0.767**	1.150	1.217	1.098	0.964	0.717	1.138	1.017	0.980	0.866	0.610
h=12	0.843	0.940	1.021	1.042	1.018	2.004	2.027	1.697	1.428	1.054	1.872	1.689	1.503	1.274	0.882
h=18	0.966	0.968	1.028	1.059	1.049	2.595	2.565	2.105	1.749	1.299	2.474	2.259	1.971	1.665	1.149
h=24	1.127	1.042	1.046	1.069	1.055	3.004	2.958	2.461	2.071	1.600	2.905	2.676	2.317	1.960	1.387
FSN															
h=1	0.467	0.266	0.289	0.305	0.284	0.319	**0.287**	**0.334**	**0.334**	0.299	**0.341**	**0.245**	**0.323**	**0.294**	0.300
h=6	0.730	0.782	0.867	0.903	0.844	**1.094**	**1.169**	**1.034**	**0.932**	0.688	**1.031**	**0.978**	**0.952**	**0.830**	0.632
h=12	1.004	1.031	1.133	1.189	1.123	2.026	**2.017**	1.670	1.432	1.031	**1.769**	**1.633**	**1.454**	**1.219**	0.886
h=18	1.157	1.083	1.159	1.232	1.168	2.655	2.593	2.134	1.809	1.310	**2.393**	**2.209**	**1.937**	**1.636**	1.143
h=24	1.325	1.173	1.195	1.256	1.172	3.058	2.980	2.490	2.128	1.610	**2.852**	**2.644**	**2.302**	**1.953**	1.368

4 Conclusion

In this paper we have developed a maximum likelihood procedure for imposing smoothing restrictions on the loading matrix of a dynamic factor model. We have used cubic spline functions to introduce smoothness in factor loadings. For a newly updated time series panel of unsmoothed Fama-Bliss zero yields for U.S. treasuries, we show that it is possible to construct a parsimonious dynamic factor model with smooth factor loadings. The number of parameters in the loading matrix of the dynamic factor model is more or less halved. Despite of this reduction in the number of parameters we find that the in-sample fit of our model is qualitatively the same as for the most general dynamic factor model. We can rotate the factor loadings in such a way that the factors are given the level, slope and curvature interpretation of the Nelson-Siegel yield curve. Our forecasting study has shown that smooth dynamic factor models are highly competitive in producing precise forecasts of the yield curve for a range of forecast horizons, from 1 month to 24 months.

Although the analysis of the U.S. term structure of interest rates is highly relevant in finance and economics, we emphasize that dynamic factor models with smooth factor loadings can be used in different settings. In many applications of the dynamic factor model it is possible to identify variables of which the factor loadings can reasonably be assumed to behave as smooth functions. An example is the modelling and forecasting of intra-daily electricity load consumption curves. Our methodology provides means to build parsimonious dynamic factor models for even high dimensional time series panels and with factors that can be given a clear interpretation. We will explore this methodology further in future work.

Appendix

The dynamic factor model is given by equations (1), (2) and (3) for a panel of N time series and r factors. When we introduce lagged factors in the observation equation (1), the model becomes

$$y_t = \mu_y + \Lambda_0 f_t + \Lambda_1 f_{t-1} + \ldots + \Lambda_s f_{t-s} + \varepsilon_t,$$

where Λ_m is an $N \times r$ loading matrix for $m = 0, 1, \ldots, s$ and where $f_t = Z\alpha_t$ and α_t remain specified as (2) and (3), respectively, for some pre-fixed integer $s > 0$. This model can still be written in state space after some modifications. We do not want to increase the state vector unnecessarily and therefore we propose the following formulation. An efficient state space representation for the model with lagged factors can be based on the state vector as

defined by

$$\alpha_t^* = \left(\alpha_t' \, , \, f_{t-1}' \, , \, \ldots \, , \, f_{t-s+1}' \, , \, f_{t-s}' \right)' ,$$

where α_t remains as in (3). For the state vector α_t^*, the observation equation becomes

$$y_t = \mu_y + \left(\Lambda_0 Z \, , \, \Lambda_1 \, , \, \ldots \, , \, \Lambda_{s-1} \, , \, \Lambda_s \right) \alpha_t^* + \varepsilon_t,$$

and the state updating equation for α_t^* becomes

$$\alpha_{t+1}^* = \begin{pmatrix} \mu_y \\ 0 \\ 0 \\ \vdots \\ 0 \end{pmatrix} + \begin{bmatrix} T & 0 & 0 & \cdots & 0 & 0 \\ Z & 0 & 0 & \cdots & 0 & 0 \\ 0 & I & 0 & \cdots & 0 & 0 \\ \vdots & & \ddots & & & \vdots \\ 0 & 0 & 0 & & I & 0 \end{bmatrix} \alpha_t^* + \begin{bmatrix} R \\ 0 \\ 0 \\ \vdots \\ 0 \end{bmatrix} \eta_t,$$

for $t = 1, \ldots, n$. This representation illustrates the generality of the state space form for dynamic factor models. The dimension of the state vector α_t^* remains relatively small since we augment α_t^* by lagged f_t's rather than lagged α_t's.

References

Bai, J. (2003). Inferential theory for factor models of large dimensions. *Econometrica 71*, 135–72.

Bliss, R. (1997). Movements in the term structure of interest rates. *Federal Reserve Bank of Atlanta Economic Review 82*, 16–33.

Bowsher, C. and R. Meeks (2008). The dynamics of economic functions: modeling and forecasting the yield curve. *J. American Statistical Association 103*, 1419–37.

Box, G. E. P., G. M. Jenkins, and G. C. Reinsel (1994). *Time Series Analysis, Forecasting and Control* (3rd ed.). San Francisco: Holden-Day.

Christensen, J., F. Diebold, and S. Rudebusch (2010). The affine arbitrage-free class of Nelson-Siegel term structure models. *J. Econometrics (forthcoming)*.

Clements, M. P. and D. Hendry (1998). *Forecasting Economic Time Series*. Cambridge: Cambridge University Press.

Connor, G. and R. A. Korajczyk (1993). A test for the number of factors in an approximate factor model. *Journal of Finance 48*(4), 1263–91.

De Pooter, M. (2007). Examining the Nelson-Siegel class of term structure models. Tinbergen Institute Discussion Paper.

Diebold, F. and C. Li (2006). Forecasting the term structure of government bond yields. *J. Econometrics 130*, 337–64.

Diebold, F., S. Rudebusch, and S. Aruoba (2006). The macroeconomy and the yield curve. *J. Econometrics 131*, 309–38.

Doz, C., D. Giannone, and L. Reichlin (2006). A quasi maximum likelihood approach for large approximate dynamic factor models. Discussion paper, CEPR.

Duffee, G. (2009). Forecasting with the term structure: The role of no-arbitrage restrictions. Working paper.

Durbin, J. and S. J. Koopman (2001). *Time Series Analysis by State Space Methods*. Oxford: Oxford University Press.

Engle, R. F. (1984, July). Wald, likelihood ratio, and lagrange multiplier tests in econometrics. In *Handbook of Econometrics*, Volume 2 of *Handbook of Econometrics*, Chapter 13, pp. 775–826. Elsevier.

Engle, R. F. and M. W. Watson (1981). A one-factor multivariate time series model of metropolitan wage rates. *J. American Statistical Association 76*, 774–81.

Fama, E. F. and R. R. Bliss (1987). The information in long-maturity forward rates. *American Economic Review 77*, 680–92.

Fengler, M., W. Haerdle, and P. Schmidt (2002). The analysis of implied volatilities. In W. Haerdle, T. Kleinow, and G. Stahl (Eds.), *Applied Quantitative Finance: Theory and Computational Tools*, Chapter 6, pp. 127–37. Berlin: Springer.

Forni, M., M. Hallin, M. Lippi, and L. Reichlin (2000). The generalized dynamic factor model: Identification and estimation. *Rev. Economics and Statistics 82*, 540–54.

Geweke, J. (1977). The dynamic factor analysis of economic time series. In D. J. Aigner and A. S. Goldberger (Eds.), *Latent variables in socio-economic models*. Amsterdam: North-Holland.

Gregory, A., A. Head, and J. Raynauld (1997). Measuring world business cycles. *International Economic Review 38*, 677–701.

Harvey, A. C. and S. J. Koopman (1993). Forecasting hourly electricity demand using time-varying splines. *J. American Statistical Association 88*, 1228–36.

Jungbacker, B. and S. J. Koopman (2008). Likelihood-based analysis for dynamic factor models. Tinbergen Institute Discussion Paper.

Koopman, S. J. and J. Durbin (2000). Fast filtering and smoothing for multivariate state space models. *J. Time Series Analysis 21*, 281–96.

Koopman, S. J., M. Mallee, and M. Van der Wel (2010). Analyzing the term structure of interest rates using the dynamic Nelson-Siegel model with time-varying parameters. *J. Business and Economic Statist. 28*, 329–343.

Koopman, S. J. and N. Shephard (1992). Exact score for time series models in state space form. *Biometrika 79*, 823–6.

Lengwiler, Y. and C. Lenz (2010). Intelligible factors for the yield curve. *J. Econometrics (forthcoming)*.

Litterman, R. and J. Scheinkman (1991). Common factors affecting bond returns. *Journal of Fixed Income 1*(1), 54–61.

Monahan, J. F. (2001). *Numerical methods of statistics*. Cambridge: Cambridge University Press.

Nelson, C. and A. Siegel (1987). Parsimonious modelling of yield curves. *Journal of Business 60-4*, 473–89.

Nocedal, J. and S. J. Wright (1999). *Numerical Optimization*. New York: Springer Verlag.

Park, B., E. Mammen, W. Haerdle, and S. Borak (2009). Time Series Modelling with Semiparametric Factor Dynamics. *J. American Statistical Association 104*, 284–98.

Poirier, D. J. (1976). *The Econometrics of Structural Change: with Special Emphasis on Spline Functions*. Amsterdam: North-Holland.

Quah, D. and T. J. Sargent (1993). A dynamic index model for large cross sections. In J. H. Stock and M. Watson (Eds.), *Business cycles, indicators and forecasting*, pp. 285–306. Chicago: University of Chicago Press.

Reis, R. and M. W. Watson (2010). Relative goods' prices, pure inflation, and the phillips correlation. *American Economic Journal: Macroeconomics 2*, 128–57.

Sargent, T. J. and C. A. Sims (1977). Business cycle modeling without pretending to have too much a priori economic theory. In C. A. S. et al. (Ed.), *New methods in business cycle research*. Minneapolis: Federal Reserve Bank of Minneapolis.

Stock, J. H. and M. Watson (2002). Macroeconomic forecasting using diffusion indexes. *J. Business and Economic Statist. 20*, 147–62.

Watson, M. W. and R. F. Engle (1983). Alternative algorithms for the estimation of dynamic factor, MIMIC and varying coefficient regression. *J. Econometrics 23*, 385–400.